

1 Calibration of Hydroxyacetonitrile (HOCH₂CN) and Methyl 2 isocyanate (CH₃NCO) Isomers using I⁻ Chemical Ionization 3 Mass Spectrometry (CIMS)

4
5 Zachary Finewax^{1,2,a}, Aparajeo Chattopadhyay^{1,2,b}, J. Andrew Neuman^{1,2}, James M. Roberts¹,
6 James B. Burkholder^{1,*}

7
8 ¹ Chemical Sciences Laboratory, National Oceanic and Atmospheric Administration (NOAA), Boulder, CO, USA

9 ² Cooperative Institute for Research in Environmental Sciences (CIRES), University of Colorado, Boulder, CO,
10 USA

11 ^a Present address: Air Pollution Control Division, Colorado Department of Health and Environment, Denver, CO,
12 USA

13 ^b Present address: Department of Earth and Environmental Sciences, University of Rochester, Rochester, NY, USA
14

15 *Correspondence to:* James B. Burkholder (James.B.Burkholder@noaa.gov)

16
17 **Abstract.** The toxic reduced nitrogen compound methyl isocyanate (CH₃NCO, MIC) has been
18 reported present in wildfire and bio-mass burning emissions, agricultural fumigation plumes, and
19 indoor air. Its isomer, hydroxyacetonitrile (HOCH₂CN, glycolonitrile, HAN) has not been
20 observed in the Earth's atmosphere to date. In this study, absolute sensitivity calibrations for these
21 isomers using two I⁻ chemical ionization mass spectrometry (I-CIMS) instruments, time-of-flight
22 (ToF) and quadrupole (Quad) instruments, commonly used in laboratory and field measurements,
23 were performed, for the first time, over a range of ion-molecule reactor temperature (10–40°C)
24 and I(H₂O)/I⁻ ratio (0.01–1). This study demonstrates that I-CIMS, under typical operating
25 conditions, is not sensitive to MIC with limits of detection (LOD) of >860 and >570 ppb for the
26 ToF and Quad I-CIMS instruments, respectively. Both I-CIMS instruments are, however, highly
27 sensitive to the HAN isomer with 0.3 and 3 ppt LODs for the ToF-CIMS and Quad-CIMS
28 instruments, respectively. The present results show that several recent field studies using I-CIMS
29 instrument detection have mis-attributed the C₂H₃NO signal to MIC. This study proposes that
30 HAN, rather than MIC, was most likely the C₂H₃NO isomer observed in those field studies,
31 although the source chemistry for HAN remains uncharacterized. This study demonstrates the
32 importance of applying absolute calibration standards in the identification and quantification of
33 isomeric compounds.

34

35 **1 Introduction**

36 The identification and quantitative measurement of atmospheric trace species are critical elements in the development
37 of air quality models and the establishment of environmental policies. Methyl isocyanate (CH_3NCO , MIC) and
38 hydroxyacetonitrile (HOCH_2CN , glycolonitrile, HAN) (Wolfsie, 1960) are toxic reduced nitrogen isomers present in
39 an extreme range of environments. MIC has been reported in wildfire and bio-mass burning, e.g., Koss et al. (2018),
40 and building fire emissions (Blomqvist et al., 2003), agricultural fumigation plumes (Woodrow et al., 2014), and
41 indoor air (Bekki et al., 2018), particularly where there is cigarette smoke (Moldoveanu, 2010), cooking emissions,
42 and chlorine-disinfectant use. HAN has been observed spectroscopically in interstellar space (see Zhao et al. (2021)
43 and references within), while measurements in the Earth's atmosphere have not been reported to date. The
44 atmospheric degradation of MIC leads to the formation of isocyanic acid (HNCO) (Papanastasiou et al., 2020), another
45 toxic reduced nitrogen compound. The atmospheric chemistry of the HAN isomer is not presently characterized.

46 The implementation of I^- chemical ionization mass spectrometry (I-CIMS) instruments, in particular high-
47 resolution time-of-flight mass spectrometer instruments (I-CIMS ToF-MS), has enabled high sensitivity laboratory
48 and ground-based field measurements as well as high spatial and temporal resolution in airborne field studies.
49 However, a general limitation of CIMS measurements is the inability to distinguish isomers, e.g., MIC and HAN
50 $\text{C}_2\text{H}_3\text{NO}$ isomers, without using pre-separation techniques such as gas chromatography. Field measurements of MIC
51 have been reported in outdoor (Priestley et al., 2018) and indoor (Mattila et al., 2020a; Mattila et al., 2020b; Wang et
52 al., 2022) environments using (I-CIMS) instruments, with sensitivity calibration estimated using voltage-scan
53 techniques (Mattila et al., 2020b; Wang et al., 2022) and analogy to the sensitivity of other VOC species (Priestley et
54 al., 2018).

55 The primary objective of this work was to establish sample handling and I-CIMS sensitivity calibration protocols
56 for the $\text{C}_2\text{H}_3\text{NO}$ MIC and HAN isomers. Absolute pressure and FTIR measurements were used to establish MIC
57 standards, while diffusion and infusion methods, coupled with total reactive nitrogen (N_r) methods, were used for the
58 quantification of HAN standards. Calibration measurements are presented for I-CIMS time-of-flight (ToF-CIMS) and
59 quadrupole CIMS (Quad-CIMS) mass spectrometry instruments over a range of $\text{I}(\text{H}_2\text{O})/\text{I}^-$ ratios and ion-molecule
60 reactor (IMR) temperatures. The results from this work can be applied to similar instruments used in laboratory and
61 field studies, although instrument sensitivities may vary somewhat depending on instrument configuration and
62 operating conditions. This work demonstrates that the recent field measurements reported by Priestley et al. (2018),
63 Mattila et al. (2020a), and Wang et al. (2022) have mis-attributed their measured I-CIMS signal, which was assigned
64 to MIC, when it was most likely due to HAN.

65 **2 Experimental Methods**

66 A primary goal of this work was the development of measurement protocols for hydroxyacetonitrile (HOCH_2CN ,
67 HAN) and methyl isocyanate (CH_3NCO , MIC) using iodide chemical ionization mass spectrometry (I-CIMS) with a
68 time-of-flight mass spectrometer (ToF-CIMS) (Lee et al., 2014) and quadrupole mass spectrometer (Quad-CIMS)
69 (Neuman et al., 2000) instruments. We have focused on calibration measurements for ToF-CIMS and Quad-CIMS
70 instruments for which calibrations for MIC and HAN have not been performed previously. An emphasis in this work
71 was placed on MIC and HAN sample handling and quantification, i.e., knowing what the sample concentration is at
72 the instrument inlet.

73 MIC and HAN samples for calibration measurements were prepared using dilute gas mixtures prepared using
74 absolute pressure measurements, diffusion sources, and infusion sources that are described in detail below. Absolute
75 concentrations were determined using FTIR spectroscopy (MIC) and a total reactive nitrogen (N_r) instrument (HAN).
76 Calibration measurements were performed with ToF- and Quad-CIMS instruments to evaluate differences in
77 sensitivity for instruments with different configurations, e.g., ion-molecule reactor (IMR) geometries, ionization
78 sources, and ion focusing optics. In addition, sensitivities were determined for a range of IMR temperature (10–40°C)
79 and $I(H_2O)/I$ ratios, commonly used in laboratory and field studies, which are known to affect I-CIMS sensitivity
80 (see Robinson et al. (2022)). The MIC and HAN calibration methods, N_r instrument and methods, and ToF- and
81 Quad-CIMS instruments are described below.

82 **2.1 Methyl isocyanate source and calibration**

83 Methyl isocyanate (MIC) is a stable volatile liquid at room temperature with a vapor pressure of ~467 hPa (1 hPa =
84 0.75 Torr) at 25°C. For the present study, a MIC sample was obtained commercially in pure form. Dilute gas-phase
85 methyl isocyanate (MIC) samples were prepared manometrically at a total pressure of 1066 hPa in a 12 L Pyrex bulb
86 with He bath gas. The MIC mixing ratio was ~3.5%. The MIC mixing ratio was also determined by Fourier transform
87 infrared spectroscopy using the absorption cross section data measured in Papanastasiou et al. (2020) from this
88 laboratory. Dilute high-pressure gas standards were prepared by diluting glass bulb standards into aluminum cylinders
89 and filled with zero air. Methyl isocyanate bulb and aluminum cylinder standards were quantitatively added to the
90 zero air flow sampled by the I-CIMS instruments.

91 **2.2 Hydroxyacetonitrile (HAN) source and calibration methods**

92 HAN is a stable semi-volatile compound, vapor pressure of 1.33 hPa at 336 K (NIOSH), that is available commercially
93 as a 70 wt% mixture with H_2O . Over the course of this study, liquid-to-gas-phase diffusion and infusion methods
94 were applied for the delivery of gas-phase HAN to the N_r calibration and I-CIMS instruments.

95 The diffusion source is described in detail elsewhere (Roberts et al., 2010; Williams et al., 2000). Basically, a
96 capillary diffusion cell regulated vapor from the liquid sample into the gas stream feeding into the N_r and I-CIMS
97 instruments. The concentration of source compound is regulated by varying the total gas flow, i.e., dilution factor.
98 This source method requires an independent determination of the compound concentration in the gas stream. The
99 infusion method has been used previously in our laboratory and is described in detail elsewhere (Bernard et al., 2017;
100 Bernard et al., 2018). Basically, a syringe pump is used to deliver a constant liquid flow (0.01–0.3 $\mu\text{L min}^{-1}$ in our
101 experiments) of a HAN sample into the gas stream feeding into the N_r and I-CIMS instruments. The region of the
102 liquid-gas interface was heated (40 to 60°C) to ensure uniform volatilization and minimize potential sample
103 condensation. Measurements were performed using the commercially available stock HAN solution and a HAN
104 sample diluted in acetone, prepared off-line. The mixing ratio of HAN in the gas flow can in principle be calculated
105 using the calibrated gas and liquid flow rates, the density of the compound, and its liquid mixing ratio, although in
106 this work, the HAN infusion source was calibrated using a total reactive nitrogen, N_r , measurement.

107 **2.3 Total reactive nitrogen, N_r , measurement**

108 The infusion source gas-phase concentration of HAN was determined by a total reactive nitrogen, N_r , measurement.
109 Total reactive nitrogen is defined as all reduced and oxidized nitrogen-containing compounds with the exception of

110 N₂ and N₂O. The N_r instrument has been demonstrated for both gas-phase and particle-phase N_r, and is described in
111 detail elsewhere (Stockwell et al., 2018). In this study, the nitrogen containing compounds in a gas-phase sample are
112 first catalytically converted on a 750°C Pt catalyst to NO and NO₂. The NO₂ is subsequently converted to NO on a
113 molybdenum oxide catalyst at 350°C. The NO then reacts with an excess of O₃ to form NO₂, which is detected by
114 chemiluminescence (Williams et al., 1998). The N_r instrument was calibrated using commercial dilute mixtures of
115 NO (5.18 ppm) and HCN (9.5 ppm) in a N₂ bath gas. HCN and NO calibrations performed over the course of the
116 study agreed to within 3%. The total flow through the N_r instrument was set to 1.048 sLPM (standard liter per minute)
117 and the total zero air flow from the infusion source was 2.148 sLPM. The excess flow passed through an exhaust line.
118 Considering uncertainties in the standards and flow rates, the 2σ uncertainty in the N_r calibration of the HAN source
119 was estimated to be 15%. The HAN infusion source was calibrated by measuring the N_r concentration as a function
120 of the liquid injection flow rate. Over the course of the study, multiple calibration experiments were performed using
121 independently prepared HAN samples.

122 2.4 Iodide Chemical Ionization Mass Spectrometry (I-CIMS)

123 I-CIMS has the ability to measure sub-part per trillion (ppt) gas-phase concentrations of organic acids, halogens,
124 oxidized organic compounds, and N₂O₅ at up to 10 Hz resolution (Huey, 2007; Neuman et al., 2000; Veres et al.,
125 2020). This relatively soft ionization technique usually yields an I⁻ cluster ion with the intact analyte molecule. I-
126 CIMS is highly selective, with the sensitivity to an analyte is dependent on the binding enthalpy of the compound with
127 I⁻. Time-of-flight mass spectrometers typically contain ion focusing quadrupoles that can also impart changes to the
128 sensitivity of analytes due to mass-dependent ion transmission and collision-induced dissociation (Robinson et al.,
129 2022). The I-CIMS instruments used in the present study have been described in detail previously and only pertinent
130 details are described below.

131 2.4.1 Time-of-Flight Chemical Ionization Mass Spectrometer (ToF-CIMS)

132 The ToF-CIMS is setup with a pressure-controlled inlet, ion molecule reactor (IMR), small segmented quadrupole
133 (SSQ), big segmented quadrupole (BSQ), and time-of-flight (ToF) mass analyzer (Veres et al., 2020). A Kr lamp
134 provided vacuum ultraviolet radiation at 124 and 117 nm that photoionized CH₃I to produce I⁻ in the IMR
135 (Breitenlechner et al., 2022; Ji et al., 2020). Analytes (A) react with I⁻ or I(H₂O)⁻ to form adducts:



138 with I-C₂H₃NO⁻ detected at m/z 183.9265. Key instrument conditions that impact the sensitivity for an analyte are the
139 IMR temperature and I(H₂O)⁻/I⁻ ratio (Lee et al., 2014; Robinson et al., 2022; Veres et al., 2020). In this study, the
140 IMR was temperature controlled between 20 and 40°C and the I(H₂O)⁻/I⁻ ratio was dynamically controlled at 0.01,
141 i.e., dry, and over the range 0.4 to 0.6, which represents a typical range of operating conditions of laboratory and field
142 instruments. The ToF-CIMS inlet was pressure controlled at 130 hPa and the flow into the inlet was controlled to 6
143 sLPM. The IMR was pressure controlled to 44 hPa (Zhang and Zhang, 2021). The pressure in the SSQ and BSQ
144 were 1.7 and 0.013 hPa, respectively. The sum of I⁻ + I(H₂O)⁻ was typically 5MHz in these experiments.

145 2.4.2 Quadrupole Chemical Ionization Mass Spectrometer (Quad-CIMS)

146 The Quad-CIMS instrument setup consisted of a critical orifice inlet (600 μm dia.) combined with an IMR, ion
147 focusing lenses, and a quadrupole mass analyzer (Neuman et al., 2000). I^- ions were generated by passing a 0.1%
148 CH_3I in N_2 mixture through a ^{210}Po radioactive source. The IMR was temperature controlled between 10 and 30°C .
149 The $\text{I}(\text{H}_2\text{O})^-/\text{I}^-$ ratio was adjusted between 0.01–1.0 by controlling the humidity of the gas flow into the CIMS, which
150 ranged from 4.2 to 4.5 sLPM. This system did not have an intermediate pressure zone between the IMR and mass
151 spectrometer chamber, common to many I-CIMS instruments, that would serve as a collisional-dissociation chamber.
152 The pressure in the IMR was maintained at 37 hPa by varying the pumping speed. The mass resolution of the Quad-
153 CIMS instrument is ~ 200 and that of the ToF-CIMS is ~ 5000 . The sum of $\text{I}^- + \text{I}(\text{H}_2\text{O})^-$ was typically 500 kHz in these
154 experiments.

155 2.5 Materials

156 Synthetic air (zero grade), N_2 (UHP, 99.999%), He (UHP, 99.999%) gases and CH_3I (99%) and acetone (99%) were
157 used as provided. Standard dilute mixtures of NO (5.18 ppm in N_2) and HCN (9.5 ppm in N_2) were obtained
158 commercially. Hydroxyacetonitrile (HAN, $\sim 70\%$ in H_2O , CAS RN: 107-16-4) and methyl isocyanate (MIC, 97+%,
159 CAS RN: 624-83-9) samples were obtained commercially. The MIC sample contained a $<3\%$ trimethylchlorosilane
160 (CAS RN: 75-77-4) inhibitor. The HAN and MIC samples were degassed in freeze—pump—thaw cycles. Samples
161 were stored in a chemical refrigerator in vacuum sealed Pyrex reservoirs prior to use.

162 A dilute (3.48%) gas mixture of MIC in He was prepared manometrically in a 12 L Pyrex bulb. Fourier transform
163 infrared spectroscopy (FTIR) measurements (1 cm^{-1} resolution, 425 cm pathlength) using a previously determined
164 absorption spectrum from our laboratory (Papanastasiou et al., 2020) confirmed the mixing ratio, to within 10% of the
165 manometric preparation. Standard dilute solutions of HAN in acetone were prepared volumetrically using 1.0–2.0 μL
166 of the commercial HAN solution and 5.0 or 10.0 mL of acetone. The standard solutions were stored in a chemical
167 refrigerator in vacuum sealed Pyrex reservoirs. Samples used in the calibration infusion experiments were extracted
168 from the standard solution with a gas-tight 10 or 100 μL syringe.

169 3. Results and Discussion

170 3.1 Methyl isocyanate (CH_3NCO , MIC)

171 ToF-CIMS and Q-CIMS measurements with MIC mixing ratios of up to 860 ppb yielded no measurable signal for the
172 I-MIC^- or $\text{I}(\text{H}_2\text{O})\text{-MIC}^-$ adducts above the background (1σ background noise level of 3 ncps). Measurements were
173 performed over the range of CIMS conditions described in the experimental section. The sensitivity upper-limits
174 obtained are given in **Table 1**, and represent the signal increase (normalized to 1 million cps of the sum of $\text{I}^- + \text{I}(\text{H}_2\text{O})^-$)
175 per mixing ratio unit increase of the compound). Our measurements indicate that MIC mixing ratios of greater than
176 1 ppm may be required to generate a detectable I-CIMS signal, if MIC can be detected by I-CIMS at all.

177 **Table 1.** ToF-CIMS and Quad-CIMS instrument sensitivity (S) and limits of detection (LOD) measured in this work
178 for hydroxyacetonitrile (HOCH_2CN , HAN) and methyl isocyanate (CH_3NCO , MIC) for typical field operating
179 conditions with an IMR temperature of 30°C , $\text{I}(\text{H}_2\text{O})^-/\text{I}^-$ ratio of 0.55, and 1 s integration. See **Fig. 3** for sensitivity
180 dependence on operating conditions.

	CH_3NCO (MIC)		HOCH_2CN (HAN)	
Instrument	S	LOD	S	LOD

	(ncps ppb ⁻¹)	(ppb)	(ncps ppt ⁻¹)	(ppt)
ToF-CIMS	<0.009	>860	19.6 ± 0.5	0.3
Quad-CIMS	<0.044	>570	25.8 ± 0.7	3

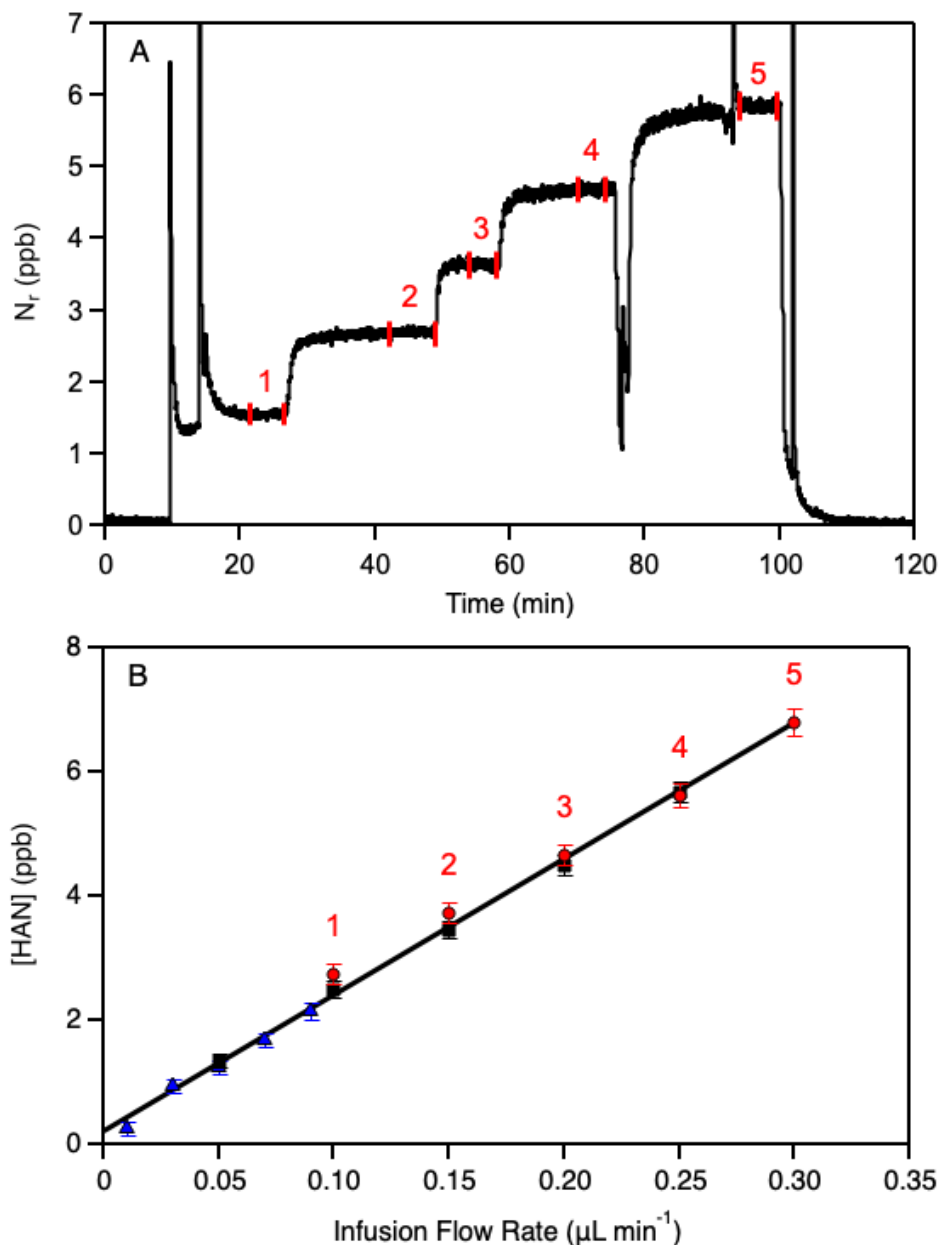
181 The ToF- and Quad-CIMS instruments used in the present study were found to be insensitive to the detection of
182 CH₃NCO (MIC). The lack of MIC sensitivity for both instruments suggests that the I⁻ cluster with MIC is not
183 thermodynamically stable in the IMR. The ion focusing or ion optics in the ToF-CIMS and the Quad-CIMS are,
184 however, quite different. The ToF-CIMS SSQ was set to 1.7 hPa, so collisions occur in this region, resulting in some
185 collisional dissociation. The BSQ focuses ions and can also result in fragmentation of I⁻ clusters. The ion optics of
186 the Quad-CIMS uses only static electric fields in a low-pressure region (<1.3 × 10⁻⁴ hPa) and does not have sufficient
187 frequency to dissociate I⁻ clusters. Given the lack of sensitivity of both ToF- and Quad-CIMS instruments to MIC, it
188 is unlikely that other common I-CIMS instrument configurations have the sensitivity to detect MIC at atmospherically
189 relevant mixing ratios.

190 3.2 Hydroxyacetonitrile (HOCH₂CN, HAN)

191 The diffusion source, with the commercial 70% HAN/H₂O solution, proved to be an unsuccessful HAN delivery
192 method. This method produced high gas-phase concentrations of an HCN impurity as identified by I-CIMS. Although
193 HCN was a minor sample impurity, <1%, its high vapor pressure (862 hPa at 295 K (Perry and Porter, 1926)) and low
194 Henry's law coefficient (~9 M Atm⁻¹ (Burkholder et al., 2019)), resulted in a [HCN]/[HAN] gas-phase mixing ratio
195 of greater than 1000, i.e., HAN was not detectable by I-CIMS using this source. The high gas-phase HCN
196 concentration, using the diffusion method, precluded quantitative calibration of HAN concentration using the total
197 reactive nitrogen calibration method.

198 The infusion source did not produce detectable gas-phase HCN above the detection limit of the mass spectrometers,
199 i.e., the HCN impurity level was much less than 1%. Therefore, HCN did not influence the absolute HAN calibration
200 determination using the N_r instrument. The region around the infusion source was heated to 50°C when using the
201 commercially available HAN stock solution. Although this source worked, it didn't provide a stable HAN signal to
202 within 10%. This source, using a dilute HAN/acetone mixture with the region of the infusion source heated to 45°C,
203 i.e., slightly below the boiling point of acetone, yielded more stable HAN signals with variations of a few percent.
204 Measurements performed at temperatures greater than 45°C yielded reasonable results, but the signal was less stable
205 due most likely to boiling of the acetone solvent.

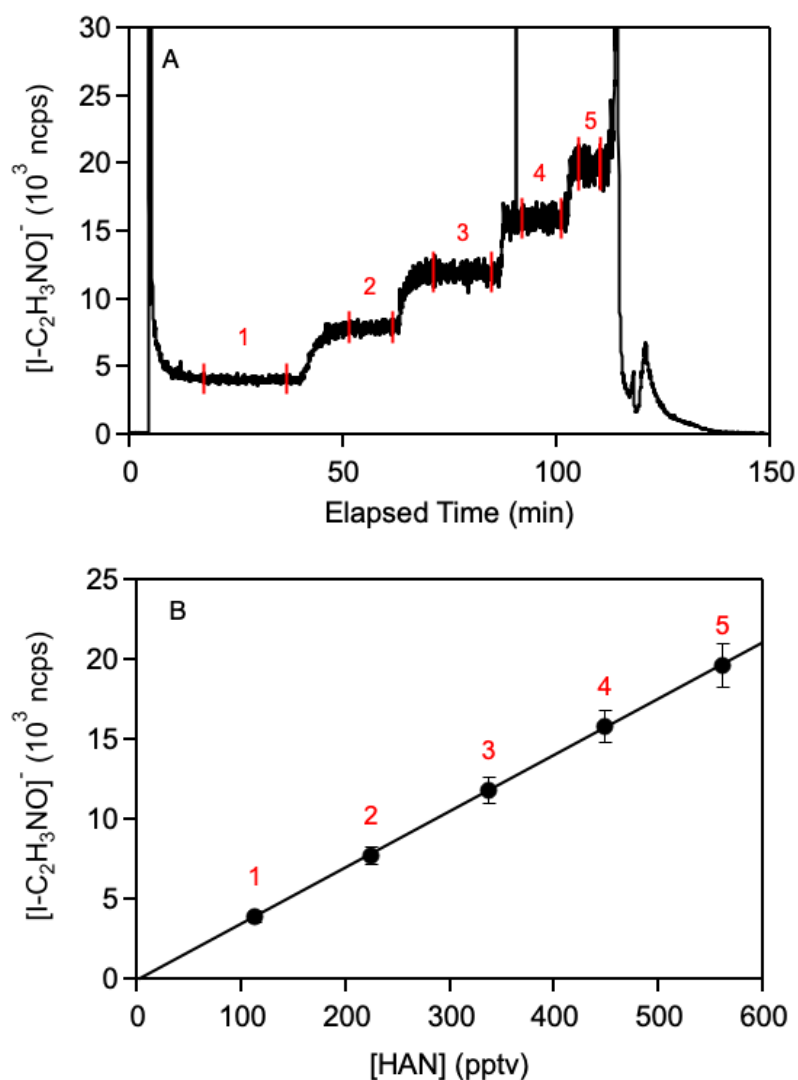
206 Calibration of hydroxyacetonitrile (HAN) solutions by total reactive nitrogen (N_r) is shown in **Fig. 1**. The infusion
207 method produces a stable source of HAN with a high signal-to-noise ratio for a typical calibration experiment. The
208 total HAN concentration was set by adjusting the injection flow rate. Individual solutions were calibrated multiple
209 times, as shown in **Fig. 1**. The 2σ uncertainty of the fit precision of [HAN] vs. infusion flow rate was determined to
210 be 4%. The small positive intercept may be due to minor unidentified N_r impurities.



211

212 **Figure 1:** Calibration of the hydroxyacetonitrile (HOCH_2CN , HAN) infusion source at 23°C using the total nitrogen, N_r , instrument
 213 (see text for details of the N_r instrument). (a) Background-corrected time series of a representative calibration experiment. The
 214 data within the numbered vertical lines were averaged and correspond to the numbered points in panel b. (b) Calibration of the
 215 HAN mixing ratio, taking the N_r measured mixing ratio, example in panel A, to be equal to the HAN mixing ratio, as a function of the
 216 infusion source flow rate. Different symbols represent independent calibration experiments. The line is an unweighted linear least-
 217 squares fit of all the data. Error bars represent 2σ measurement precision.

218 Calibrations of the HAN signal on the ToF-CIMS and Quad-CIMS instruments were made by varying the infusion
 219 flow rate, see representative data for the Quad-CIMS in **Fig. 2**. The obtained ToF- and Quad-CIMS sensitivity for
 220 HAN given in **Table 1** was obtained using the infusion method with the dilute HAN/acetone samples. For typical
 221 field operating conditions with an IMR temperature of 30°C , $I(\text{H}_2\text{O})/I^-$ ratio of 0.55, and 1 s integration the HAN
 222 sensitivity of the ToF I-CIMS was determined to be ~ 20 ncps ppt $^{-1}$.



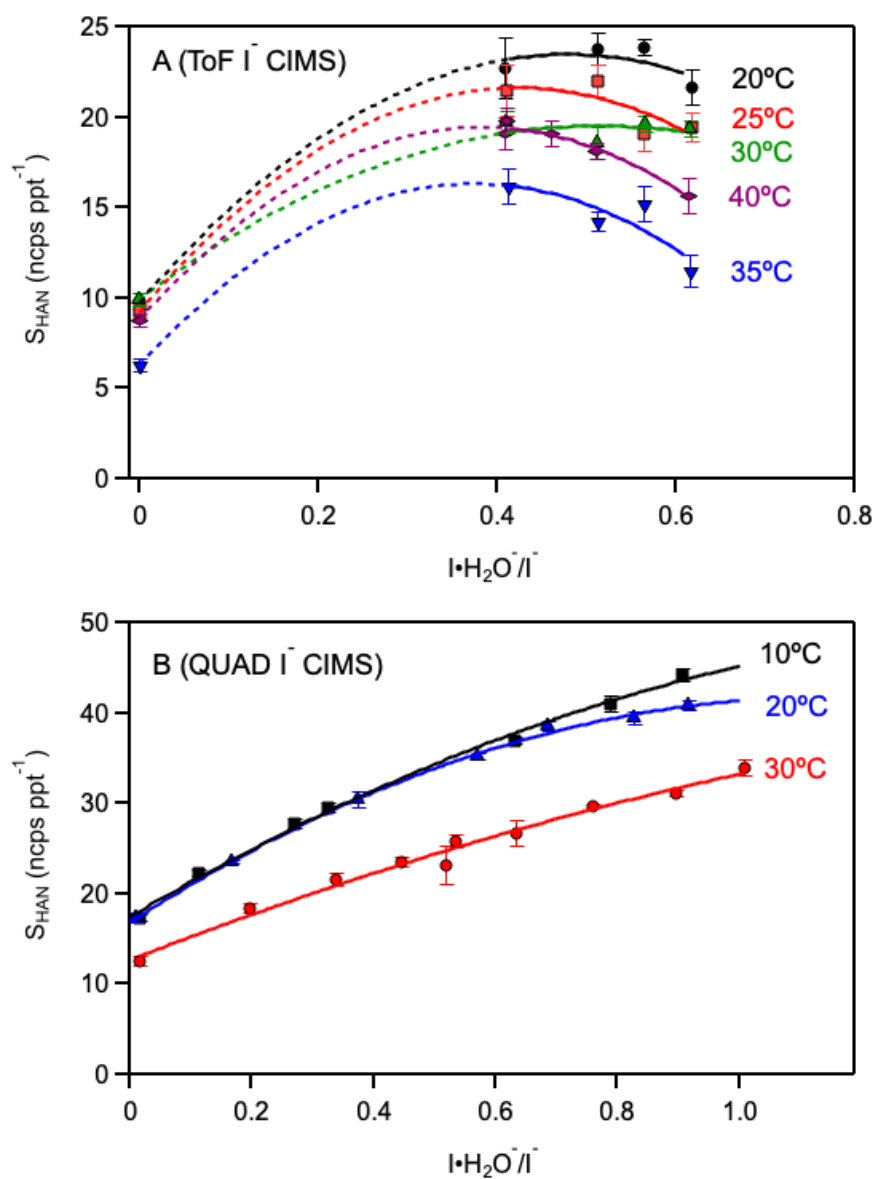
223
 224 **Figure 2:** Calibration of the Quad-CIMS instrument using the hydroxyacetonitrile (HOCH₂CN, HAN) infusion source at 23°C
 225 (see text for details of the Quad-CIMS instrument). (a) Background-corrected time series of a representative Quad-CIMS
 226 calibration experiment (IMR temperature = 20°C, I(H₂O)/I⁻ = 0.57). The data within the numbered vertical lines were averaged
 227 and correspond to the numbered points in panel B. (b) Quad-CIMS HAN calibration curve where the HAN concentration was
 228 determined from the N_r calibration of the infusion source, e.g., see Fig. 1. The line is an unweighted linear least-squares fit of the
 229 data. Error bars represent 2σ measurement precision.

230 The HAN concentration from the infusion source at the instrument inlet was varied, for each IMR temperature and
 231 I(H₂O)/I⁻ ratio, to determine the HAN sensitivity temperature and I(H₂O)/I⁻ dependence shown in Fig. 3. The ToF-
 232 CIMS and Quad-CIMS instruments are both highly sensitive to HAN, but displayed slightly different temperature and
 233 I(H₂O)/I⁻ dependencies. As the temperature increased, the HAN sensitivity decreased consistent with the [I-HAN]⁻
 234 adduct being less stable at higher temperatures. For the ToF-CIMS instrument, the HAN sensitivity decreased a factor
 235 of ~1.5–2 between 20 and 40°C at the highest I(H₂O)/I⁻ ratio included in this study. For the Quad-CIMS instrument,
 236 a ~25% decrease in HAN sensitivity was observed at a I(H₂O)/I⁻ ratio of 1 when increasing the IMR temperature from
 237 10 to 30°C. The I(H₂O)/I⁻ dependency for HAN sensitivity was fit reasonably well with a quadratic dependence on
 238 I(H₂O)/I⁻: $A + B(I(H_2O)/I^-) - C(I(H_2O)/I^-)^2$, where the constant term represents HAN clustering with I⁻, reaction 1;
 239 the linear term represents HAN undergoing a ligand switching reaction with I(H₂O)⁻, reaction 2; and the quadratic
 240 term may represent a lack of reactivity of higher-order H₂O clusters, I(H₂O)_n⁻ where n > 1 or a shift in the

241 $(\text{I-HAN})^- + \text{H}_2\text{O} \leftrightarrow (\text{I-H}_2\text{O})^- + \text{HAN}$

(3)

242 equilibrium.



243
244 **Figure 3:** Hydroxyacetonitrile (HOCH_2CN , HAN) calibration factors for the ToF and QUAD mass spectrometers used in this
245 work as a function of the $\text{I}(\text{H}_2\text{O})^-/\text{I}^-$ ratio and ion-molecule reactor, IMR, temperature. Error bars represent 2σ precision of the
246 linear calibration fits. Lines are empirical polynomial fits to guide the eye. (a) HAN calibration factors measured for the ToF-
247 CIMS. Symbols represent IMR temperatures of 20°C (black circles), 25°C (red squares), 30°C (green triangles), 35°C (blue upside-
248 down triangles), and 40°C (purple diamonds). (b) Quad-CIMS HAN calibration data. Symbols represent IMR temperatures of:
249 10°C (black squares), 20°C (blue triangles), 30°C (red circles).

250 There is a plausible explanation for the differences in the Quad-CIMS and ToF-CIMS instrument $I(\text{H}_2\text{O})/\text{I}^-$
251 sensitivity dependence. First, there are differences in these instruments in the ion focusing downstream of the IMR.
252 The ToF-CIMS contains an SSQ at 1.73 hPa that imparts an electric field and acts as a collisional dissociation chamber.
253 The subsequent BSQ also imparts an electric field that can dissociate weakly bound I^- clusters. The $I(\text{H}_2\text{O})/\text{I}^-$ is
254 dynamically controlled in the ToF-CIMS by what is observed at the detector. Therefore, the $I(\text{H}_2\text{O})^-$ (and $I(\text{H}_2\text{O})_n^-$)
255 ion counts are not representative of the $I(\text{H}_2\text{O})/\text{I}^-$ ratio in the IMR, i.e., the $I(\text{H}_2\text{O})/\text{I}^-$ ratio in the IMR is being under-
256 estimated, although we were unable to quantify the dependence. The Quad-CIMS, which has ion lenses at low-
257 pressure downstream of the IMR, $1.3\text{--}0.13 \times 10^{-3}$ hPa, should have only minor collisional dissociation, if any.
258 Therefore, the $I(\text{H}_2\text{O})/\text{I}^-$ ratio measured by the Quad-CIMS is, most likely, close to the actual $I(\text{H}_2\text{O})/\text{I}^-$ in the IMR.
259 In conclusion, it is recommended that instruments used to quantify HAN be calibrated under actual operating
260 conditions. The protocols presented in this work can be used for the calibration of HAN.

261 4 Conclusions

262 In this study, protocols for determining I-CIMS instrument sensitivity for CH_3NCO (MIC) and HOCH_2CN (HAN),
263 two stable toxic $\text{C}_2\text{H}_3\text{NO}$ isomers (Panda et al., 2023), were developed. Calibration of ToF-CIMS and Quad-CIMS
264 instruments for HAN were performed over a range of instrument conditions commonly used in laboratory and field
265 experiments, including: ion molecule reactor (IMR) temperature ($10\text{--}40^\circ\text{C}$) and $I(\text{H}_2\text{O})/\text{I}^-$ ratios between 0.1 and 1.
266 Both I-CIMS instruments were found to be highly sensitive to HAN with 0.3 and 3 ppt limits of detection (LOD) for
267 the ToF-CIMS and Quad-CIMS instruments, respectively, for measurements with the IMR at 30°C , $I(\text{H}_2\text{O})/\text{I}^-$ ratio of
268 0.55, and 1 s integration (see **Table 1**). The instruments were insensitive to MIC with LODs of >860 and >570 ppb
269 for the ToF and Quad I-CIMS instruments, respectively. A weak negative temperature dependence and systematic
270 positive $I(\text{H}_2\text{O})/\text{I}^-$ ratio dependence was observed for HAN. The ToF and Quad I-CIMS instruments have similar
271 normalized sensitivities, reflecting the similar chemistry in the ion molecule reaction regions. The ToF instrument
272 has much lower LOD because the reagent ion concentration was approximately 10 times greater than that in the Quad
273 instrument and the ToF has far better mass resolution. The results from this study should, to a first approximation,
274 translate to other laboratory and field I-CIMS instruments.

275 Our work demonstrates that the previous field studies of Priestley et al. (2018), Mattila et al. (2020a; 2020b), and
276 Wang et al. (2022), which used I-CIMS detection methods, mis-attributed the $\text{C}_2\text{H}_3\text{NO}$ mass signal as methyl
277 isocyanate, MIC, and also provides evidence for the observation of HAN, a previously unrecognized species in these
278 environments. Our results suggest that HAN was observed, but do not imply that MIC was not present in the
279 environments studied by Priestley et al., Mattila et al., and Wang et al. Since I-CIMS is not sensitive to MIC,
280 alternative measurement methods, such as proton transfer CIMS, would be required to identify the presence of MIC.
281 Our work indicates that HAN is likely to be present in the troposphere. Iyer et al. (2016) and Hyttinen et al. (2018)
282 provide an explanation for the significant difference in the I-CIMS sensitivity for MIC (CH_3NCO) and HAN
283 (HOCH_2CN), due to the I- cluster binding energies. That is, the H-bonding with the HO group in HAN leads to a
284 stable I- cluster, while MIC would not form a stable I- cluster.

285 The heterogeneous and gas-phase atmospheric chemistry of HOCH_2CN (HAN) are, however, not presently
286 characterized. Here, we postulate that in addition to primary HAN emissions, e.g., from wildfires, that HAN would
287 be formed heterogeneously in clouds, or on hydrated aerosol, via the liquid-phase reaction:



289 The partitioning of HAN between the liquid- and gas-phase will depend on its Henry's law coefficient, which has not
290 been measured to date. Sander (2023) reports an estimated Henry's law coefficient value of $\sim 130 \text{ M atm}^{-1}$, using a
291 quantitative structure-property relationship, which implies partitioning of HAN into the gas-phase. HCN and H₂CO
292 are ubiquitous in the atmosphere with elevated concentrations in wildfire plumes, which may lead to a significant
293 enhancement of the HAN concentration following a wildfire plume exposure to clouds. Our work will aid future
294 laboratory and field studies to identify the atmospheric source chemistry of HAN as well as its atmospheric loss
295 processes and degradation products.

296 *Data availability.* NA

297 *Author contributions.* ZF undertook the experimental measurements and contributed to the first draft and writing of
298 the paper. AC performed the MIC infrared measurements and initial ToF MIC measurements. JAN performed the
299 initial ToF MIC measurements. JMR performed the initial Nr measurements and contributed to the writing of the
300 paper. JBB supervised the project and completed the writing of the paper.

301 *Competing interests.* The authors declare that they have no conflict of interest.

302 *Financial support.* This research was supported in part by the NOAA Climate Goal and NASA Atmospheric
303 Composition Programs.

304 Review statement.

305

- 307 Bekki, K., Uchiyama, S., and Kunugita, N.: Analysis of isocyanates in indoor dust, *Anal. Bioanal. Chem.*, 410,
308 4247-4251, <https://doi.org/10.1007/s00216-018-1110-y>, 2018.
- 309 Bernard, F., Papanastasiou, D. K., Papadimitriou, V. C., and Burkholder, J. B.: Infrared absorption spectra of linear
310 (L2-L5) and cyclic (D3-D6) permethylsiloxanes, *J. Quant. Spectros. Rad. Trans.*, 202, 247-254,
311 <https://doi.org/10.1016/j.jqsrt.2017.08.006>, 2017.
- 312 Bernard, F., Papanastasiou, D. K., Papadimitriou, V. C., and Burkholder, J. B.: Infrared absorption spectra of
313 $N(C_xF_{2x+1})_3$, $x = 2-5$ perfluoroamines, *J. Quant. Spectrosc. Rad. Trans.*, 211, 166-171,
314 <https://doi.org/doi:10.1016/j.jqsrt.2018.02.039>, 2018.
- 315 Blomqvist, P., Hertzberg, T., Dalene, M., and Skarping, G.: Isocyanates, aminoisocyanates and amines from fires - a
316 screening of common materials found in buildings, *Fire Mater.*, 27, 275-294,
317 <https://doi.org/doi:10.1002/fam.836>, 2003.
- 318 Breitenlechner, M., Novak, G. A., Neuman, J. A., Rollins, A. W., and Veres, P. R.: A versatile vacuum ultraviolet
319 ion source for reduced pressure bipolar chemical ionization mass spectrometry, *Atmos. Meas. Tech.*, 15, 1159-
320 1169, <https://doi.org/doi:10.5194/amt-15-1159-2022>, 2022.
- 321 Burkholder, J. B., Sander, S. P., Abbatt, J., Barker, J. R., Cappa, C., Crouse, J. D., Dibble, T. S., Huie, R. E., Kolb,
322 C. E., Kurylo, M. J., Orkin, V. L., Percival, C. J., Wilmouth, D. M., and Wine, P. H.: "Chemical Kinetics and
323 Photochemical Data for Use in Atmospheric Studies, Evaluation No. 19," JPL Publication 19-5, Jet Propulsion
324 Laboratory, Pasadena, 2020 <http://jpldataeval.jpl.nasa.gov>, 2019.
- 325 Huey, L. G.: Measurement of trace atmospheric species by chemical ionization mass spectrometry: speciation of
326 reactive nitrogen and future directions, *Mass Spectrom. Rev.*, 26, 166-184,
327 <https://doi.org/doi:10.1002/mas.20118>, 2007.
- 328 Hyttinen, N., Otkjaer, R. V., Iyer, S., Kjaergaard, H. G., Rissanen, M. P., Wennberg, P. O., and Kurten, T.:
329 Computational comparison of different reagent ions in the chemical ionization of oxidized multifunctional
330 compounds, *J. Phys. Chem. A.*, 122, 269-279, <https://doi.org/10.1021/acs.jpca.7b10015>, 2018.
- 331 Iyer, S., Lopez-Hilfiker, F., Lee, B. H., Thornton, J. A., and Kurten, T.: Modeling the detection of organic and
332 inorganic compounds using iodide-based chemical ionization, *J. Phys. Chem. A*, 120, 576-587,
333 <https://doi.org/10.1021/acs.jpca.5b09837>, 2016.
- 334 Ji, Y., Huey, G., Tanner, D. J., Lee, Y. R., Veres, P. R., Neuman, J. A., Wang, Y. H., and Wang, X. M.: A vacuum
335 ultraviolet ion source (VUV-IS) for iodide-chemical ionization mass spectrometry: a substitute for radioactive
336 ion sources, *Atmos. Meas. Tech.*, 13, 3683-3696, <https://doi.org/doi:10.5194/amt-13-3683-2020>, 2020.
- 337 Koss, A. R., Sekimoto, K., Gilman, J. B., Selimovic, V., Coggon, M. M., Zarzana, K. J., Yuan, B., Lerner, B. M.,
338 Brown, S. S., Jimenez, J. L., Krechmer, J., Roberts, J. M., Warneke, C., Yokelson, R. J., and de Gouw, J.: Non-
339 methane organic gas emissions from biomass burning: identification, quantification, and emission factors from
340 PTR-ToF during the FIREX 2016 laboratory experiment, *Atmos. Chem. Phys.*, 18, 3299-3319,
341 <https://doi.org/10.5194/acp-18-3299-2018>, 2018.
- 342 Lee, B. H., Lopez-Hilfiker, F. D., Mohr, C., Kurten, T., Worsnop, D. R., and Thornton, J. A.: An iodide-adduct
343 high-resolution time-of-flight chemical-ionization mass spectrometer: Application to atmospheric inorganic and
344 organic compounds, *Environ. Sci. Technol.*, 48, 6309-6317, <https://doi.org/doi:10.1021/es500362a>, 2014.
- 345 Mattila, J. M., Arata, C., Wang, C., Katz, E. F., Abeleira, A., Zhou, Y., Zhou, S., Goldstein, A. H., Abbatt, J. P. D.,
346 DeCarlo, P. F., and Farmer, D. K.: Dark chemistry during bleach cleaning enhances oxidation of organics and
347 secondary organic aerosol production indoors, *Environ. Sci. Tech. Lett.*, 7, 795-801,
348 <https://doi.org/10.1021/acs.estlett.0c00573>, 2020a.
- 349 Mattila, J. M., Lakey, P. S. J., Shiraiwa, M., Wang, C., Abbatt, J. P. D., Arata, C., Goldstein, A. H., Ampollini, L.,
350 Katz, E. F., DeCarlo, P. F., Zhou, S., Kahan, T. F., Cardoso-Saldaña, F. J., Ruiz, L. H., Abeleira, A., Boedicker,
351 E. K., Vance, M. E., and Farmer, D. K.: Multiphase chemistry controls inorganic chlorinated and nitrogenated
352 compounds in indoor air during bleach cleaning, *Environ. Sci. Tech.*, 54, 1730-1739,
353 <https://doi.org/10.1021/acs.est.9b05767>, 2020b.
- 354 Moldoveanu, S. C.: Analysis of acrylonitrile and α -methacrylonitrile in vapor phase of mainstream cigarette smoke
355 using a charcoal trap for collection, *Contrib. Tobac. Res.*, 24, <https://doi.org/10.2478/cttr-2013-0892>, 2010.
- 356 Neuman, J. A., Gao, R. S., Schein, M. E., Ciciora, S. J., Holecek, J. C., Thompson, T. L., Winkler, R. H.,
357 McLaughlin, R. J., Northway, M. J., Richard, E. C., and Fahey, D. W.: A fast-response chemical ionization mass
358 spectrometer for in situ measurements of HNO_3 in the upper troposphere and lower stratosphere, *Rev. Sci.*
359 *Instrum.*, 71, 3886-3894, <https://doi.org/doi:10.1063/1.1289679>, 2000.
- 360 NIOSH. Glycolonitrile National Institute Occupational Safety Health.
- 361 Panda, S., Chiranjibi, A., Awasthi, D., Ghoshal, S., and Anoop, A.: Exploring the chemical space of C_2H_3NO
362 isomers and bimolecular reactions with hydrogen cyanide and formaldehyde: Insights into the emergence of life,
363 *Earth Space Chem.*, 7, 1739-1752, <https://doi.org/10.1021/acsearthspacechem.3c00113>, 2023.

364 Papanastasiou, D. K., Bernard, F., and Burkholder, J. B.: Atmospheric fate of methyl isocyanate, CH₃NCO: OH and
365 Cl reaction kinetics and identification of formyl isocyanate, HC(O)NCO, *Earth Space Chem.*, 4, 1626-1637,
366 <https://doi.org/10.1021/acsearthspacechem.0c00157>, 2020.

367 Perry, J. H., and Porter, F.: The vapor pressures of solid and liquid hydrogen cyanide, *J. Amer. Chem. Soc.*, 48, 297-
368 300, 1926.

369 Priestley, M., Le Breton, M., Bannan, T. J., Leather, K. E., Bacak, A., Reyes-Villegas, E., De Vocht, F., Shallcross,
370 B. M. A., Brazier, T., Khan, M. A., Allan, J., Shallcross, D. E., Coe, H., and Percival, C. J.: Observations of
371 isocyanate, amide, nitrate, and nitro compounds from an anthropogenic biomass burning using a Tof-CIMS, *J.*
372 *Geophys. Res.*, 123, 7687-7704, <https://doi.org/10.1002/2017jd027316>, 2018.

373 Roberts, J. M., Veres, P., Warneke, C., Neuman, J. A., Washenfelder, R. A., Brown, S. S., Baasandorj, M.,
374 Burkholder, J. B., Burling, I. R., Johnson, T. J., Yokelson, R. J., and de Gouw, J.: Measurement of HONO,
375 HNCO, and other inorganic acids by negative-ion proton-transfer chemical-ionization mass spectrometry (NI-
376 PT-CIMS): application to biomass burning emissions, *Atmospheric Measurement Techniques*, 3, 981-990,
377 <https://doi.org/10.5194/amt-3-981-2010>, 2010.

378 Robinson, M. A., Neuman, J. A., Huey, L. G., Roberts, J. M., Brown, S. S., and Veres, P. R.: Temperature-
379 dependent sensitivity of iodide chemical ionization mass spectrometers, *Atmos. Meas. Tech.*, 15, 4295-4305,
380 <https://doi.org/10.5194/amt-15-4295-2022>, 2022.

381 Sander, R.: Compilation of Henry's law constants (version 5.0.0) for water as solvent, *Atmos. Chem. Phys.*, 23,
382 10901-12440, <https://doi.org/doi:10.5194/acp-23-10901-2023>, 2023.

383 Stockwell, C. E., Kupc, A., Witkowski, B., Talukdar, R. K., Liu, Y., Selimovic, V., Zarzana, K. J., Sekimoto, K.,
384 Warneke, C., Washenfelder, R. A., Yokelson, R. J., Middlebrook, A. M., and Roberts, J. M.: Characterization of
385 a catalyst-based conversion technique to measure total particulate nitrogen and organic carbon and comparison to
386 a particle mass measurement instrument, *Atmos. Meas. Tech.*, 11, 2749-2768, <https://doi.org/10.5194/amt-11-2749-2018>, 2018.

388 Veres, P. R., Neuman, J. A., Bertram, T. H., Assaf, E., Wolfe, G. M., Williamson, C. J., Weinzierl, B., Tilmes, S.,
389 Thompson, C. R., Thames, A. B., Schroder, J. C., Saiz-Lopez, A., Rollins, A. W., Roberts, J. M., Price, D.,
390 Peischl, J., Nault, B. A., Moller, K. H., Miller, D. O., Meinardi, S., Li, Q. Y., Lamarque, J. F., Kupc, A.,
391 Kjaergaard, H. G., Kinnison, D., Jimenez, J. L., Jernigan, C. M., Hornbrook, R. S., Hills, A., Dollner, M., Day,
392 D. A., Cuevas, C. A., Campuzano-Jost, P., Burkholder, J., Bui, T. P., Brune, W. H., Brown, S. S., Brock, C. A.,
393 Bourgeois, I., Blake, D. R., Apel, E. C., and Ryerson, T. B.: Global airborne sampling reveals a previously
394 unobserved dimethyl sulfide oxidation mechanism in the marine atmosphere, *Proc. Nat. Acad. Sci.*, 117, 4505-
395 4510, <https://doi.org/10.1073/pnas.1919344117>, 2020.

396 Wang, C., Mattila, J. M., Farmer, D. K., Arata, C., Goldstein, A. H., and Abbatt, J. P. D.: Behavior of isocyanic acid
397 and other nitrogen-containing volatile organic compounds in the indoor environment, *Environ. Sci. Tech.*, 56,
398 7598-7607, <https://doi.org/10.1021/acs.est.1c08182>, 2022.

399 Williams, E. J., Baumann, K., Roberts, J. M., Bertman, S. B., Norton, R. B., Fehsenfeld, F. C., Springston, S. R.,
400 Nunnermacker, L. J., Newman, L., Olszyna, K., Meagher, J., Hartsell, B., Edgerton, E., Pearson, J. R., and
401 Rodgers, M. O.: Intercomparison of ground-based NO_y measurement techniques, *J. Geophys. Res.*, 103, 22261-
402 22280, doi: 22210.21029/22298JD00074, 1998.

403 Williams, J., Roberts, J. M., Bertman, S. B., Stroud, C. A., Fehsenfeld, F. C., Baumann, K., Buhr, M. P., Knapp, K.,
404 Murphy, P. C., Nowick, M., and Williams, E. J.: A method for the airborne measurement of PAN, PPN, and
405 MPAN, *J. Geophys. Res.*, 105, 28943-28960, <https://doi.org/Doi.10.1029/2000jd900373>, 2000.

406 Wolfsie, J. H.: Glycolonitrile toxicity, *J. Occup. Med.*, 2, 588-590, 1960.

407 Woodrow, J. E., LePage, J. T., Miller, G. C., and Hebert, V. R.: Determination of methyl isocyanate in outdoor
408 residential air near metam-sodium soil fumigations, *J. Agr. Food Chem.*, 62, 8921-8927,
409 <https://doi.org/10.1021/jf501696a>, 2014.

410 Zhang, W., and Zhang, H. F.: Secondary ion chemistry mediated by ozone and acidic organic molecules in iodide-
411 adduct chemical ionization mass spectrometry, *Anal. Chem.*, 93, 8595-8602,
412 <https://doi.org/10.1021/acs.analchem.1c01486>, 2021.

413 Zhao, G., Quan, D., Zhang, X., Feng, G., Zhou, J., Li, D., Meng, Q., Chang, Q., Yang, X., He, M., and Ma, M.-S.:
414 Glycolonitrile (HOCH₂CN) chemistry in star-forming regions, *Astrophys. J. Supp. Series*, 257, 26,
415 <https://doi.org/doi:10.3847/1538-4365/ac17ee>, 2021.

416

417